

Evolutionary combinatorial chemistry, a novel tool for SAR studies on peptide transport across the blood–brain barrier. Part 2. Design, synthesis and evaluation of a first generation of peptides[‡]

MERITXELL TEIXIDÓ,^a IGNASI BELDA,^a ESTHER ZURITA,^a XAVIER LLORÀ,^b MYRIAM FABRE,^c SENÉN VILARÓ,^d FERNANDO ALBERICIO^{a,e} and ERNEST GIRALT^{a,e*}

^a Institut de Recerca Biomèdica de Barcelona (IRBB-PCB), Parc Científic de Barcelona, Josep Samitier, 1-5. E-08028, Barcelona, Spain

^b Illinois Genetic Algorithms Laboratory, Department of General Engineering, University of Illinois, IL 61801, USA

^c Advancell, Parc Científic de Barcelona, Universitat de Barcelona, Spain

^d Celltec UB, Departament Biologia Cel·lular, Universitat de Barcelona, Spain

^e Departament de Química Orgànica, Universitat de Barcelona, Martí i Franquès, 1. E-08028, Barcelona, Spain

Received 20 January 2005; Revised 10 March 2005; Accepted 22 February 2005

Abstract: The use of high-throughput methods in drug discovery allows the generation and testing of a large number of compounds, but at the price of providing redundant information. Evolutionary combinatorial chemistry combines the selection and synthesis of biologically active compounds with artificial intelligence optimization methods, such as genetic algorithms (GA). Drug candidates for the treatment of central nervous system (CNS) disorders must overcome the blood–brain barrier (BBB). This paper reports a new genetic algorithm that searches for the optimal physicochemical properties for peptide transport across the blood–brain barrier. A first generation of peptides has been generated and synthesized. Due to the high content of *N*-methyl amino acids present in most of these peptides, their syntheses were especially challenging due to over-incorporations, deletions and DKP formations. Distinct fragmentation patterns during peptide cleavage have been identified. The first generation of peptides has been studied by evaluation techniques such as immobilized artificial membrane chromatography (IAMC), a cell-based assay, $\log P_{\text{octanol/water}}$ calculations, etc. Finally, a second generation has been proposed. Copyright © 2005 European Peptide Society and John Wiley & Sons, Ltd.

Keywords: genetic algorithm; blood–brain barrier; peptide transport; *N*-methyl amino acids

INTRODUCTION

Many peptides with therapeutic potential for the treatment of central nervous system (CNS) disorders

Abbreviations: Abbreviations used for amino acids and the designation of peptides follow the rules of the IUPAC-IUB Commission of Biochemical Nomenclature listed in *J. Peptide Sci.* 2003; **9**: 1–8. The following additional abbreviations are used: AcOH, acetic acid; Ac₂O, acetic anhydride; AM, *p*-(*R,S*)- α -{1-[(9-fluorenyl)methoxyformamido]-2,4-dimethoxybenzyl}phenoxyacetic acid; BBB, blood–brain barrier; BBEC, bovine brain endothelial cells; Barlos resin, 2-chlorotrityl chloride resin; DMEM, Dulbecco's modified Eagle medium; EDT, 1,2-ethanedithiol; GA, genetic algorithm; HBSS, Hank's balanced salt solution; IAMC, immobilized artificial membrane chromatography; $\log P_{\text{octanol/water}}$, octanol–water partition coefficient; *p*-MBHA, *p*-methylbenzhydrylamine; MeCN, acetonitrile; MeOH, methanol; PC, phosphatidylcholine; PDA, photo diode array; PyAOP, (7-azabenzotriazol-1-yl)oxy-tris(pyrrolidino)phosphonium hexafluorophosphate; TBME, *tert*-butylmethyl ether; TEER, transendothelial electrical resistance; TIS, triisopropylsilane. Amino acid symbols denote the *L* configuration unless otherwise stated. All reported solvent ratios are expressed as volume/volume unless otherwise stated.

*Correspondence to: E. Giralt, Institut de Recerca Biomèdica de Barcelona, Parc Científic de Barcelona, Josep Samitier, 1-5, E-08028 Barcelona, Spain; e-mail: egiralt@pcb.ub.es

[‡] Part 1 refers to the following publication: Teixidó M, Belda I, Roselló X, González S, Fabre M, Llorà X, Bacardit J, Garrell JM, Vilaró S, Albericio F, Giralt E. Development of a genetic algorithm to design and identify peptides that can cross the blood–brain barrier. 1. Design and validation in silico. *QSAR Comb. Sci.* 2003; **22**: 745–753.

have recently been identified [1,2]. Successful drug development requires efficient delivery to the target site. In order to reach their target sites inside the CNS these peptide drug candidates must overcome the blood–brain barrier (BBB). The blood–brain barrier is vital for the regulation of the internal environment of the brain and is present in all vertebrate brains.

The discovery of the blood–brain barrier in the late 19th century stemmed from the observation by the German bacteriologist, Paul Ehrlich, that intravenously administered dyes stain all the organs except the brain [3]. In 1913 Edwin Goldman hypothesized that cerebral capillaries provide the anatomical basis for this physiological barrier [4]. His hypothesis was confirmed by electron microscopy [5,6].

The BBB prevents the entrance of more than 98% of all potential neurotherapeutics. It is formed at the endothelial level, where tight junctions between cells avoid any paracellular pathway (Figure 1).

While several transport mechanisms occur at the BBB, this work has focused on the passive diffusion mechanism (Figure 2).

The most widely known tool for predicting absorption is probably the 'Lipinski rule of five' [7]. In addition, a wide variety of simple rules for predicting the ability of a

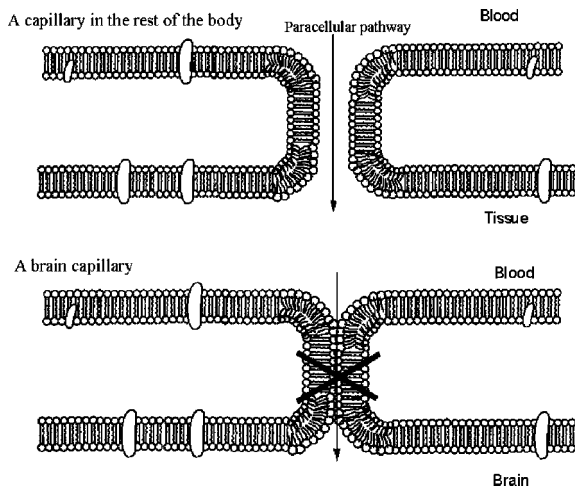


Figure 1 Schematic representations of capillary structure in the brain and in the rest of the body.

compound to cross the BBB have been established over the past 5 years [8–11]. Considering these rules, one might think that transport across the BBB is negligible for peptides larger than tripeptides, however, this is not necessarily true. In the mid-1970s, the concept that intact peptides could cross the BBB was introduced to explain the CNS effects of the administration of certain peptides [12,13]. Since then, various peptides that are able to cross the BBB by passive diffusion have been identified [14,15].

The prediction of a peptide's ability to cross the BBB is not a simple task; hence there exists the need for the rational study of the relevant factors that affect the movement across this physiological barrier. The determination of these factors will allow modifications of peptides with known therapeutic interest that could improve their entrance into the brain. Taking this objective as the aim of the project, different tools to study the physicochemical properties that enable a peptide to cross the BBB were employed.

This project is framed within the field of evolutionary combinatorial chemistry, a branch of the combinatorial chemistry inspired by natural processes of evolution. This branch uses mathematical methods of optimization, such as genetic algorithms (GA), in order to guide the search for compounds with the desired properties.

The search for these compounds is considered an evolutive process where new and better compounds are synthesized based on the properties of previously synthesized and evaluated molecules (Figure 3). It was necessary to optimize the design of this algorithm, to develop the synthetic methodology for the synthesis of these peptides, as well as to explore different tools for the evaluation of their ability to cross the blood–brain barrier. These evaluation tools may include chromatographic techniques, *in vitro* models using cells and *in vivo* methods. An overview of different aspects of the use of genetic algorithms, the synthesis of the

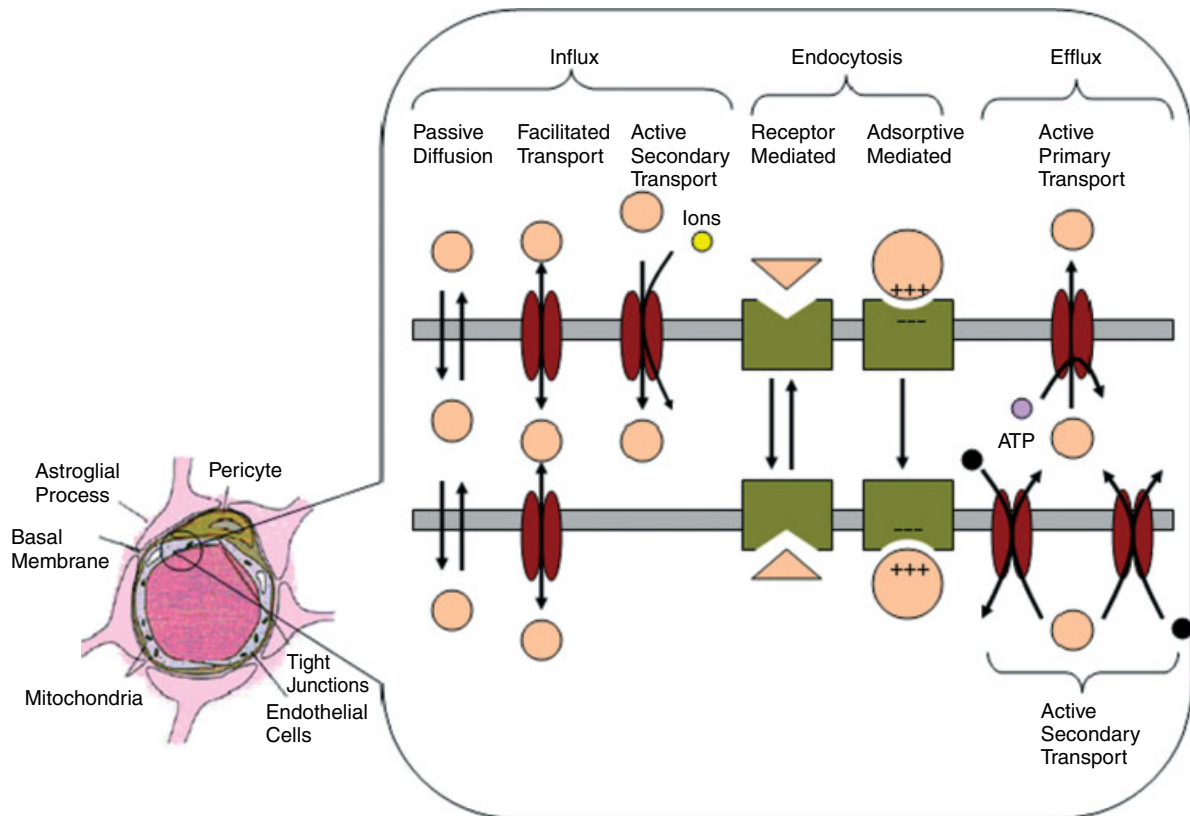


Figure 2 Transport mechanisms present in the blood–brain barrier.

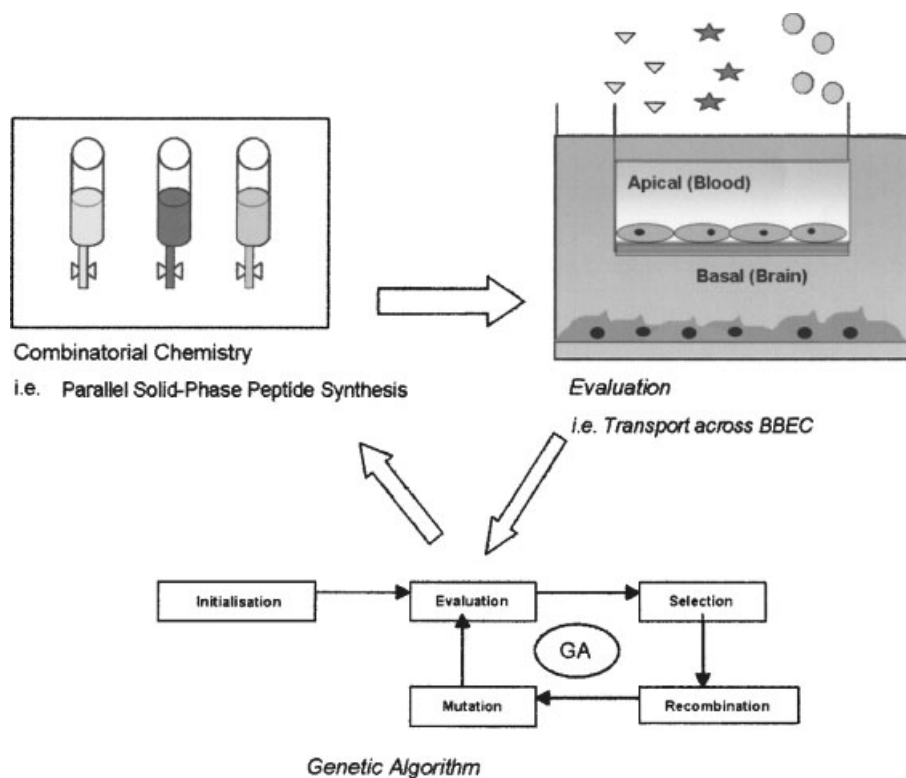


Figure 3 Scheme of the evolutive process formed by the genetic algorithm, peptide synthesis and transport evaluation.

first generation of peptides and their evaluation using different tools, is herein presented.

RESULTS AND DISCUSSION

Design and Use of a Genetic Algorithm

In terms of peptide design it was decided to explore the use of evolutionary combinatorial chemistry. In evolutionary combinatorial chemistry the selection and synthesis of biologically active compounds is combined with artificial intelligence optimization methods, such as genetic algorithms. Genetic algorithms (GA) were first proposed by Holland in 1975 [16] and they are based on Darwinian theories of natural evolution, whereby individuals with the highest degree of adaptation to their environment have the greatest chance of survival.

By eliminating redundant information, genetic algorithms are able to reduce the number of candidate solutions needed for problem solving, hence accelerating processes such as drug development. They are particularly well suited for cases where little is known about the search space.

In genetic algorithms, the candidate solutions are encoded as chromosomes. The chromosome for this study is a set of physicochemical properties, rather than a peptide sequence, believed to be relevant for the transport of peptides across the BBB.

The factors that govern whether a given peptide can cross the BBB are not fully understood, since it is

difficult to model the BBB *in vitro* [17] and comparison of data from different sources is complex. Nevertheless, there is a consensus that properties such as lipid solubility, peptide length, molecular weight, number of potential hydrogen bonds, presence of *N*-methylated and aromatic amino acids, amphiphilic nature and conformational arrangements are probably involved [18–27].

Figure 4 shows the set of physical-chemical properties that forms the chromosome for this study, including type of *C* and *N*-terminal groups, number of potential hydrogen bonds and polycationic character among others.

In Figure 5, an example of a peptide and the chromosome that encodes its characteristics is shown. For instance, the length of this heptapeptide is encoded as a value of 3 in the first position of its chromosome; the acetyl moiety corresponds to a 2 in the third position, etc.

Multiple peptides can be encoded by the same chromosome as long as they share the same set of physical-chemical properties.

Scheme 1 indicates the location of the genetic algorithm within the workflow of the study. Once the first generation of chromosomes was created by the GA, a peptide was selected for each chromosome. After the synthesis and subsequent evaluation of these peptides, a ranking was established. Based upon this ranking, the genetic algorithm determines the chromosomes of the next generation. The average and

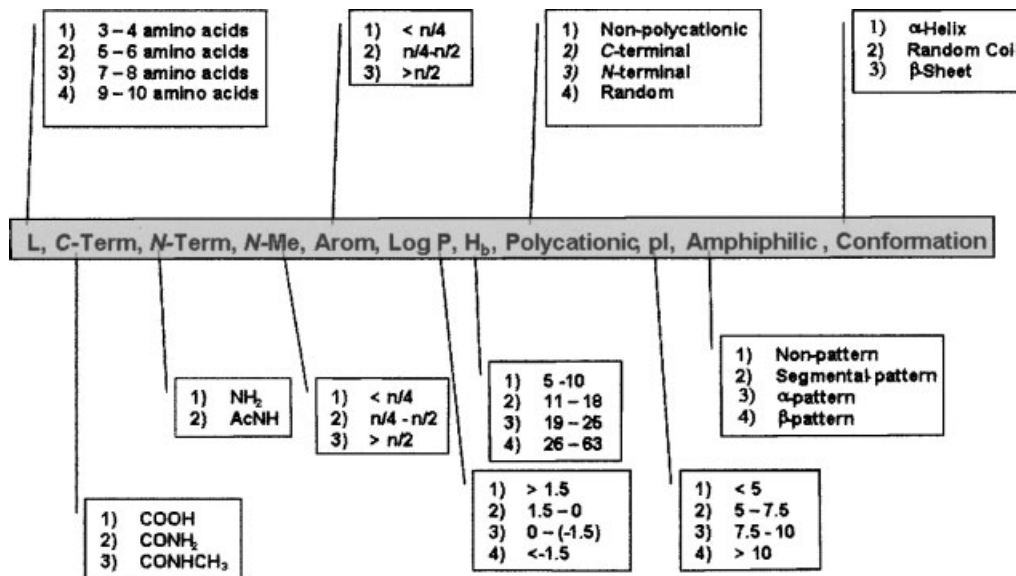


Figure 4 Chromosome description. Where *L* represents peptide length; *C-term* and *N-term* are the *C* and *N*-terminal groups of the peptide; *N-Me* is the ratio of *N*-methylated amino acid residues; *Arom* is the ratio of aromatic amino acid residues; *Log P* is the octanol–water partition coefficient; *H-Bonds* is the number of potential hydrogen bonds; *Polycationic* describes the presence of consecutive positively charged amino acids; *Amphiphilicity* describes the distribution of polar and non-polar amino acid residues; *Conformation* describes the predicted secondary structure.

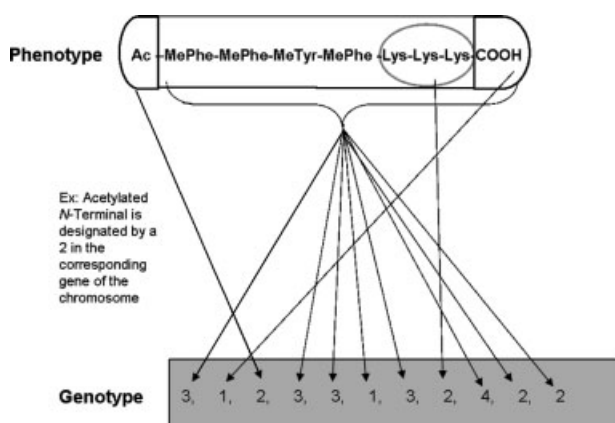


Figure 5 Example of a peptide and the chromosome that encodes the physicochemical characteristics of this peptide.

the maximal blood–brain barrier transport increase with each generation. In genetic algorithms the iterative application of some operators causes a population to evolve. These operators are involved in the selection, recombination and mutation of a population

Selection replicates the most successful solutions, recombination mixes different parts of these solutions, and mutation randomly perturbs these solutions (Figure 6).

Genetic algorithms are highly configurable tools. In order to optimize the genetic algorithm for this project, several operator parameters were fine-tuned, such as genetic algorithm geometry, percentage of replication, and the probabilities of cross-over and mutation. For a more in depth discussion of the genetic algorithm

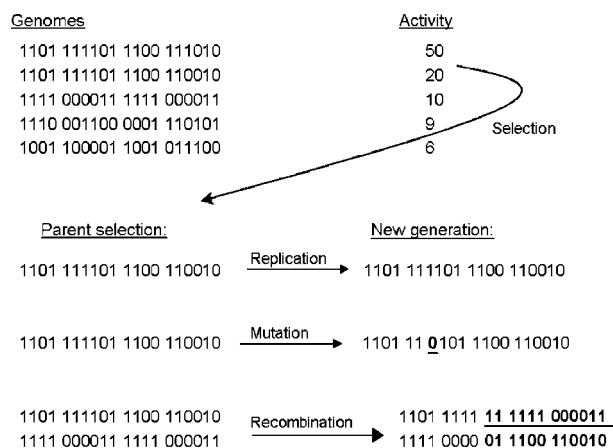
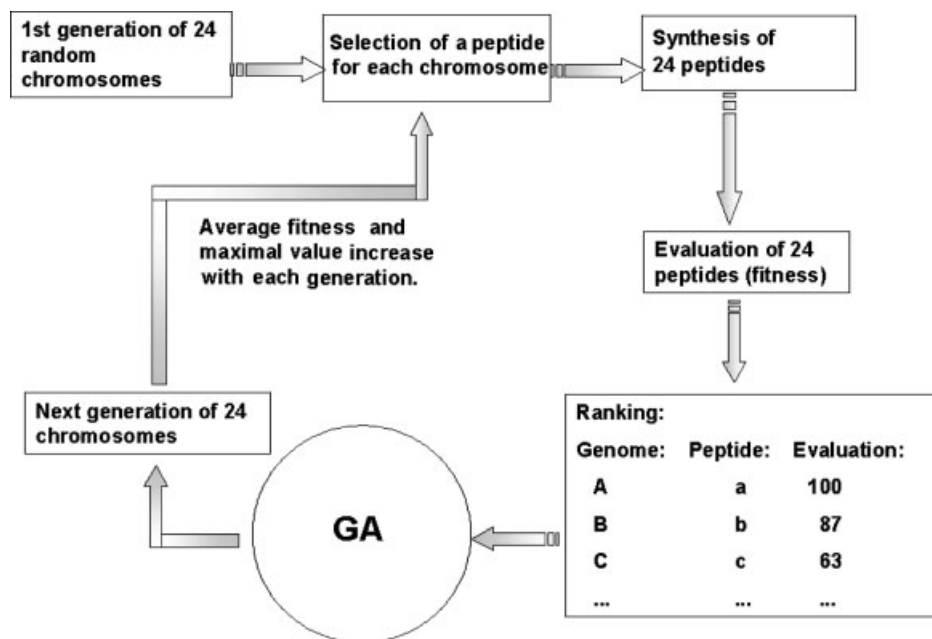


Figure 6 Scheme where the location of the genetic algorithm within the workflow can be seen.

design and fine-tuning within the project, the reader is referred to a recently published article [28].

Synthesis of the First Generation

The evolution starts with the creation and synthesis of the first generation. The first generation of chromosomes was created randomly and a peptide was selected and synthesized for each chromosome. Table 1A shows the 24 chromosomes corresponding to the first generation and Table 1B illustrates the peptide sequences corresponding to the first generation. The peptides are grouped according to their *C*-terminal groups (CONH₂, CONHCH₃, COOH).



Scheme 1 Location of the genetic algorithm within the workflow of the project.

Table 1A Chromosomes Corresponding to the First Generation

N°	Genotype
(1)	(3,2,1,1,1,3,3,1,3,3,1)
(2)	(2,2,1,1,1,4,2,1,1,1,3)
(3)	(3,2,1,3,2,2,2,1,1,4,2)
(4)	(2,2,2,3,1,1,2,1,4,3,2)
(5)	(2,2,2,3,2,3,1,1,4,3,2)
(6)	(2,2,2,1,2,3,3,1,1,3,3)
(7)	(1,2,2,1,1,4,2,1,4,3,2)
(8)	(4,2,2,1,1,4,3,1,4,2,2)
(9)	(1,2,2,3,1,3,2,1,2,1,2)
(10)	(1,2,2,1,3,2,2,1,2,4,1)
(11)	(4,3,1,1,1,4,4,4,3,1,1)
(12)	(3,3,1,2,2,1,2,1,4,4,2)
(13)	(3,3,1,3,2,2,3,2,4,1,2)
(14)	(3,3,1,1,3,3,3,1,4,1,3)
(15)	(1,3,1,2,2,4,3,1,4,1,2)
(16)	(2,3,1,2,2,4,3,1,4,1,2)
(17)	(2,3,1,1,2,1,2,1,2,2,2)
(18)	(4,3,2,3,1,3,4,2,1,1,2)
(19)	(2,3,2,1,1,3,4,2,3,1,1)
(20)	(2,1,1,3,2,2,2,1,3,2,2)
(21)	(3,1,1,2,2,2,3,3,4,1,2)
(22)	(1,1,1,1,1,4,3,1,2,3,2)
(23)	(3,1,2,3,3,1,3,1,2,3,2)
(24)	(4,1,2,3,1,4,4,4,3,2,2)

Due to the high content of *N*-methyl amino acids, the synthesis of the first generation of peptides was not trivial. Challenges encountered during the preparation of the peptide library corresponding to the first generation

have been discussed in depth in a recent article [29]. In general, different methods for the coupling of amino acids to resin-bound *N*-methyl amino acids were explored, with PyAOP and PyBOP/HOAt proving to be the most promising reagents. The use of triphosgene [30] was not considered for safety reasons. For the removal of Fmoc groups from an *N*-methyl amino acid the traditional 20% piperidine in DMF deprotection reagent was complemented by treatment of the resin with piperidine/DBU/toluene/DMF (5:5:20:70). This deprotection cocktail combines the use of a stronger base (DBU), with the resin-swelling quality of toluene. Various challenges were encountered during the synthesis of these peptides, including: over-incorporations, deletions, distinct fragmentation patterns and, in some cases, diketopiperazine (DKP) formation. Furthermore, some of the peptides gave HPLC chromatograms with multiple peaks, possibly due to a very slow *cis-trans* conformational conversion of the peptide amide bonds.

Amino acid over-incorporations were detected during the synthesis of some peptides, especially when couplings employed the pre-formed anhydride [31,32]. Deletions also occurred during the synthesis of several peptides; as a result certain couplings could not be performed with a yield higher than 50% (e.g. the coupling of *N*-methyl isoleucine to *N*-methyl isoleucine in peptide 4). The distribution of the *N*-methyl amino acids in the peptide sequence seems to be relevant, as deletions were mainly observed when *N*-methyl amino acids were located at the C-terminal (peptide 20 versus peptide 20bis). Different fragmentation patterns were identified after the TFA cleavage of the peptide-resins (Figure 7). Fragmentations occurred for peptides containing an

Table 1B Library of Peptides Corresponding to the First Generation

Peptide	Peptide sequence	N-terminal group	C-terminal group
1	Met-Cys-Glu-Val-Phe-Lys-Lys	NH ₂	CONH ₂
2	Glu-Gly-Pro-MeAsp-Gly	NH ₂	CONH ₂
2 bis	Glu-Pro-Gly-MeGlu-Gly	NH ₂	CONH ₂
3	Ile-MeAsp-MePhe-Pro-MeAla-MeGlu-MePhe	NH ₂	CONH ₂
4	Lys-Melle-Melle-Lys-MePhe	AcNH	CONH ₂
5	His-MeAla-MePhe-MeGly-MeGly	AcNH	CONH ₂
6	MeLeu-Asn-Asp-Tyr-Cys-His	AcNH	CONH ₂
6 bis	Asn-MeLeu-Asp-Tyr-Cys-His	AcNH	CONH ₂
7	Arg-MeGlu-Lys-Pro	AcNH	CONH ₂
8	His-Pro-MeGly-His-Arg-MeThr-Ala-Gly-Pro	AcNH	CONH ₂
9	MeSer-Lys-MeThr-MeAsp	AcNH	CONH ₂
9 bis	Tyr-MeAsp-MeGly-MeArg	AcNH	CONH ₂
10	Phe-Glu-Phe-His	AcNH	CONH ₂
11	MeGlu-Asp-Asn-Glu-Lys-Arg-Lys-Tyr-Ala-MeVal	NH ₂	CONHCH ₃
12	Trp-Pro-Melle-Arg-MeVal-Trp-MeLeu	NH ₂	CONHCH ₃
13	MeAla-Trp-MePhe-Lys-MeArg-Lys-MeLeu	NH ₂	CONHCH ₃
14	Phe-Phe-Lys-His-Lys-Tyr-Gly	NH ₂	CONHCH ₃
15	Tyr-MeArg-Trp-MeArg	NH ₂	CONHCH ₃
16	MePhe-Lys-His-Lys-Arg-MeAsp	NH ₂	CONHCH ₃
17	Cys-Ile-MePhe-Phe-Asp-Trp	NH ₂	CONHCH ₃
18	Melle-MeGlu-Glu-MeGlu-Phe-MeGlu-MeArg-MeArg-MeArg	AcNH	CONHCH ₃
19	MeAsp-Glu-Tyr-Lys-Lys-Lys	AcNH	CONHCH ₃
19 bis	Cys-Cys-Glu-Lys-Arg-Lys	AcNH	CONHCH ₃
20	Trp-Tyr-MeArg-MeLeu-MeGly-Melle	NH ₂	COOH
20 bis	MePhe-MeLeu-Melle-Tyr-Lys	NH ₂	COOH
21	MeLeu-MeLeu-Lys-Arg-Arg-MePhe-Phe-MePhe	NH ₂	COOH
22	Arg-Trp-Ile-Asp	NH ₂	COOH
23	MePhe-Ile-MeArg-MeSer-MePhe-Phe-Trp	AcNH	COOH
23 bis	Tyr-MePhe-Tyr-MeArg-Trp-MeAla-MeGly	AcNH	COOH
24	Gly-MeAsp-Glu-MeArg-Arg-MeArg-Melle-MeAla-Thr	AcNH	COOH
24 bis	Pro-MeGlu-MeGlu-MeArg-Arg-MeArg-MeSer-MeLeu-MeGly	AcNH	COOH

acetylated *N*-methyl amino acid at the *N*-terminal, a possible mechanism [33] for the fragmentation of Ac-*N*-methyl amino acid is proposed in Figure 7A. Fragmentation also occurred between consecutive *N*-methyl amino acids (Figure 7B). DKP formation was also a side reaction that took place during the cleavage process.

HPLC chromatograms with multiple peaks were typical of peptides with *N*-methyl amino acids distributed in a cluster close to the *C*-terminal (Figure 8). Although the presence of epimerization can not be completely excluded, this multiplicity is most likely due to a very slow *cis-trans* conformational conversion of the peptide amide bonds. The fact that reinjection of a single isolated peak also gave rise to a multiple HPLC pattern is further evidence of this conversion.

Certain peptides could not be obtained satisfactorily; in those cases other peptides (denoted by 'bis') encoded by the same chromosome were chosen and synthesized. Nevertheless, the majority of the peptides were successfully synthesized. The good yields obtained after purification for peptides 3 and 5 (44% and 33%,

respectively), which contain a high proportion of *N*-methyl residues, should be highlighted (Table 2).

Evaluation of Peptide Transport Ability

Once the first generation was obtained it was studied by several techniques, with the aim of ultimately choosing one technique for use as the evaluative tool for future generations. The techniques explored included: log $P_{\text{octanol/water}}$ calculation, HPLC RP-C₁₈ analysis, immobilized artificial membrane chromatography (IAMC) and an *in vitro* cell-based assay model incorporating bovine brain endothelial cells (BBEC).

One may consider that the ideal assay for evaluating the ability of a compound to enter the CNS is that which most closely resembles the *in vivo* situation. Other aspects such as the throughput of the experiment, the information that can be derived from the results and also certain ethical values must also be taken into account. At first glance, the ideal choice would seem to be the use of an *in vivo* assay, but the cost, the need for training and the low throughput of these

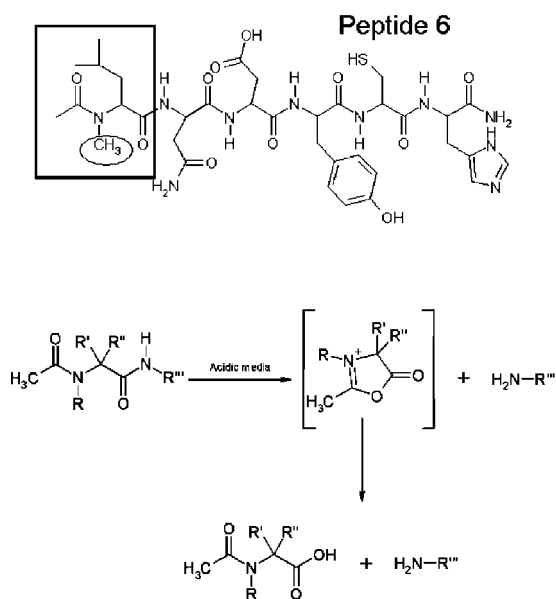
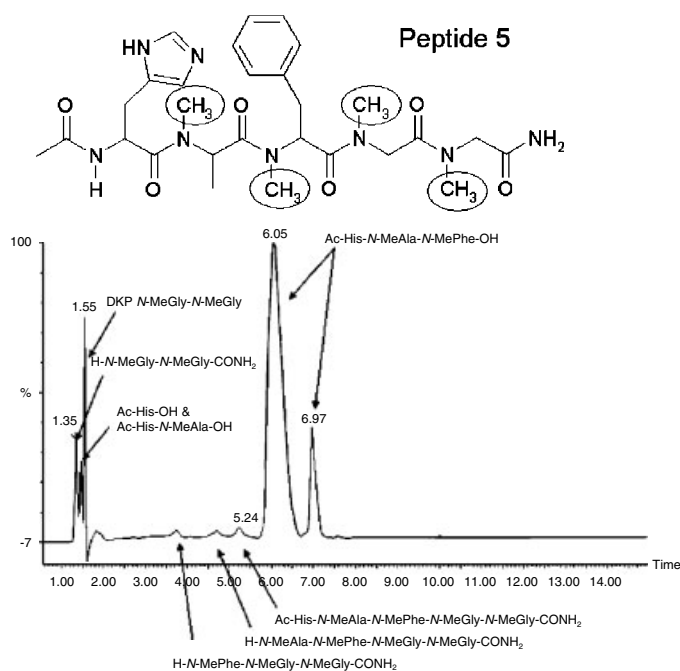
(A) Ac-MeXaa₁ aa₂-aa₃-...(B) MeXaa_{n-2} MeXaa_{n-1}-MeXaa_n-CONH₂

Figure 7 Different fragmentation patterns identified during the synthesis of the first generation of peptides.

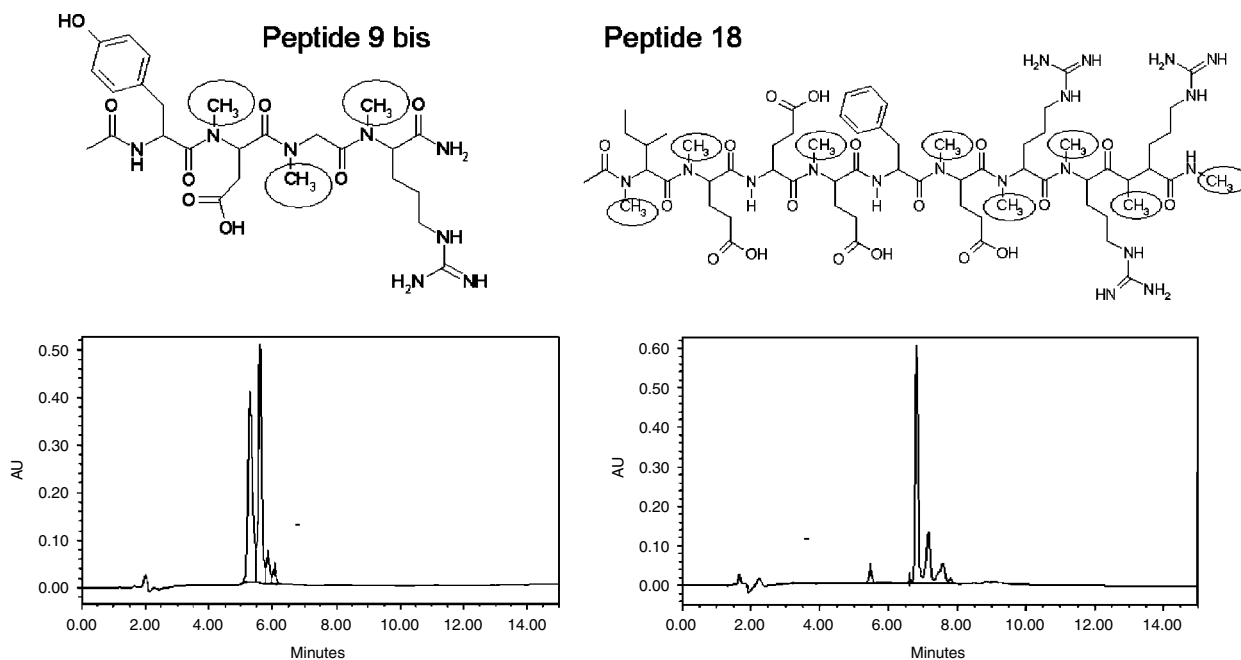


Figure 8 HPLC chromatograms of peptides with *N*-methyl amino acids distributed as a cluster close to the *C*-terminal show multiple peaks. Conditions: Symmetry C₁₈ (4.6 × 150 mm) 5 mm column, linear gradient from 5% to 50% acetonitrile (+0.036% TFA) in water (+0.045% TFA) over 15 min, 1 ml/min, detection 220 nm.

techniques must be considered. Furthermore, certain issues have yet to be resolved, for instance, the fact that most experiments are carried out in healthy animals without considering the modifications that an illness can introduce into an *in vivo* assay. It is well known that certain parameters such as protein binding, blood

flow [34] and BBB permeability may undergo changes during illness [35].

Among the *in vivo* experiments, there is an important group that is strongly linked to behavioural parameters such as analeptic effects, antidepressive effects and morphine dependence. These assays require that the

Table 2 Synthesis and Purification Yields Corresponding to the First Generation

Peptide	% Yield Synthesis and purification	Peptide	% Yield Synthesis and purification
1	72	14	11
2	—	15	2.3
2 bis	47	16	7.4
3	44	17	15
4	5.2	18	0.8
5	33	19	14
6	7.7	19 bis	11
6 bis	11	20	—
7	84	20 bis	8.5
8	26	21	12
9	—	22	87
9 bis	4.8	23	3.4
10	41	23 bis	1.1
11	3.7	24	—
12	0.9	24 bis	<0.2
13	4.9		

compound to be studied affects at least one known behavioural parameter.

Another *in vivo* technique for evaluating BBB transport is microdialysis [36], which monitors the local concentration of a compound in the extracellular fluid inside the brain. This technique still needs some validation, in addition, strict control of experimental parameters and highly skilled personnel are required. The main advantage of this technique is that it permits the study of the free drug (the active form). Due to the difficulties and disadvantages of *in vivo* assays, they were not used in this work.

The *in vitro* cellular model that has been chosen uses BBEC. This *in vitro* assay had several parameters that needed to be optimized. The use of cells implicates, among other factors, a certain low throughput due to the time needed to achieve a confluent monolayer. In both *in vivo* and *in vitro* assays, cells express a variety of transport mechanisms that may be involved in permeability. This project is focused only on passive diffusion, and for this reason methods that predict or evaluate only this transport mechanism have been used. In general terms, the method chosen to evaluate BBB transport should be simple, automatizable with high throughput, low cost and require only a small amount of test compound.

Log $P_{\text{octanol/water}}$

Due to the tight junctions between the endothelial cells of brain capillaries, the cells can be considered as a continuous lipid layer. For this reason, the solubility

of a compound in a lipidic media has historically been considered a determinant for the ability of a compound to reach the CNS by passive diffusion. This lipid solubility can be measured as a partition coefficient between an organic solvent and water. The use of partition coefficients to predict compound transport across membranes was introduced in 1899 by Meyer [37] and in 1901 by Overton [38]. They observed that the narcotic effect of certain drugs could be associated with their oil–water partition coefficient. The partition coefficient obtained between octanol and water ($\log P_{\text{octanol/water}}$) [18] has been one of the most widely used prediction methods of the transport of compounds across physiological barriers, although it has been proved that is not very reliable as a prediction tool. For hydrophobic compounds the octanol–water partition coefficient correctly correlates with the partition of a compound into a membrane [39], but for hydrophilic compounds this correlation is not as satisfactory.

In our case, peptide $\log P_{\text{octanol/water}}$ values were calculated *in silico* using the program PLOGP, developed by Tao [40]. This program predicts the $\log P_{\text{octanol/water}}$ of a peptide based on the contribution of each amino acid and also considers C or N-terminal modifications. The $\log P_{\text{octanol/water}}$ values for the first generation of peptides are shown in Table 3B.

RP-HPLC C_{18} Analysis

Liquid chromatography using octadecyl as a stationary phase (C_{18}) has been used as an alternative to $\log P_{\text{octanol/water}}$. This method has the advantage of being simple and fast, and is hence amenable to high-throughput.

The retention time (t_r) by RP-HPLC was measured using a Symmetry column C_{18} (150 × 4.6 mm) 5 μm , 100 Å, in a linear gradient of 0–100% MeCN (+0.036% TFA) in H_2O (+0.045% TFA) over 15 min, at a flow rate of 1 ml/min, with UV detection at 220 nm.

The RP-HPLC retention times (t_r) for the peptides of the first generation are shown in Table 3C.

Nevertheless, the use of this stationary phase presents certain limitations akin to those of the $\log P_{\text{octanol/water}}$ method (e.g. a weak structural similarity to the biological membrane). Octanol contains a hydrophobic tail and a hydrophilic head (OH) but the stationary phase does not have any hydrophilic moiety, it is formed only by a hydrophobic hydrocarbon chain (C_{18}). Thus, this chromatographic technique only models the partition process that is associated with the hydrophobic core of bilayers.

IAMC Analysis

In order to better mimic the structural characteristics of the cellular membrane, Katz and Diamond [41] introduced the measurement of coefficients of partition into liposome suspensions. This method has been used

Table 3 Rankings obtained for the First Generation of Peptides in the Four Different Techniques used to Evaluate Peptide Transport across the Blood–brain Barrier: (A) Bovine Brain Endothelial Capillary Cells *in vitro* assay. (B) Log $P_{\text{octanol/water}}$. (C) RP-HPLC C_{18} analysis (D) IAMC

Peptide	BBEC assay % T_{3600}	Peptide	Log $P_{\text{oct/water}}$	Peptide	HPLC (tr)	Peptide	IAMC (K_{IAM})
22	174	23	4.1	23	10.03	21	>150
3	136	4	2.4	17	9.08	4	45.1
21	110	17	2.2	12	8.17	23	35.3
2bis	104	12	1.7	3	7.50	3	23.2
23	101	21	1.3	24bis	7.45	24bis	17.8
10	89	20bis	0.8	21	6.99	1	13.0
19bis	81	13	0.6	10	6.84	11	7.2
14	74	10	0.5	20bis	6.62	15	5.4
5	71	3	0.1	6	6.43	8	4.9
15	70	19bis	-0.1	4	6.23	18	4.4
8	68	5	-0.2	13	5.98	13	3.9
18	65	14	-0.4	18	5.93	6	3.6
1	63	6	-0.4	22	5.85	20bis	3.3
11	59	1	-0.4	5	5.66	19bis	3.2
13	59	9bis	-1.3	15	5.59	10	2.0
20bis	59	18	-1.3	1	5.53	22	1.6
4	54	7	-1.8	14	5.10	5	1.2
6	53	15	-2.2	9bis	5.07	9bis	0.4
9bis	52	22	-2.2	11	4.94	7	0.4
16	49	24bis	-2.4	8	4.31	12	0.0
12	39	16	-2.5	19bis	4.30	14	-0.1
17	39	8	-2.8	7	4.27	2bis	-0.2
7	39	2bis	-4.0	16	4.26	16	-0.2
		11	-4.4	2bis	4.10	17	-0.3

in several studies and exhibits a good correlation with drug activity [42,43].

The main advantage of the liposome method is that it can model polar and non-polar interactions, but the preparation of liposome suspensions is tedious.

In the late 1980s, Pidgeon [44] developed a chromatographic technique that uses immobilized artificial membranes on solid support (IAMC, immobilized artificial membrane chromatography), in which phospholipid molecules covalently immobilized to silica particles at high density are used as the stationary phase. This technique has been used to purify membrane proteins [45], to immobilize enzymes [46] and to predict transport across biological barriers [47].

This chromatographic technique is adequate for the evaluation of peptide transport across the blood–brain barrier because it is considered a good technique to establish rankings of transport by passive diffusion. It exhibits a good correlation with *in vitro* cell based assays [48] and it is very convenient in terms of high throughput.

IAMC interactions include ionic, lipophilic and hydrogen bonding interactions that can be combined under a parameter known as phospholipophilicity.

Retention times of the first generation peptides were determined using an IAMC column with phosphatidylcholine (PC), the major phospholipid found in cell membranes, covalently immobilized (10 × 4.6 mm, 12 μm, 300 Å, IAM.PC.DD2 column, Regis Technologies Inc.). The compounds were detected by UV absorption at 220 nm. The chromatograms were obtained using an HPLC working isocratically with a mobile phase containing 10 mM phosphate buffer, 2.7 mM KCl and 137 mM NaCl at pH 7.4. No acetonitrile was used in order to mimic blood conditions.

The retention times (t_r) were transformed into capacity factors (k'_{IAM}) according to the following equation: $k'_{\text{IAM}} = (t_r - t_0)/t_0$, where t_r is the retention time of the studied compound and t_0 is the retention time of a compound that would not be retained by the column (e.g. citric acid). The k'_{IAM} values of the first generation of peptides are shown in Table 3D.

BBEC Assay

The *in vitro* cell-based assay that has been chosen uses bovine brain endothelial capillary cells (Figure 3). This model is advantageous because it exhibits many of

the characteristics of the blood–brain barrier. Compared with the physiological situation it maintains very relevant characteristics such as: (1) absence of fenestrations, (2) few pinocytotic vesicles, (3) tight intercellular junctions and (4) an abundance of mitochondria. In addition, biochemically in this assay the cells keep active enzymes such as: (1) alkaline phosphatase, (2) gamma-glutamyl transpeptidase and (3) angiotensin converting enzyme. This model also expresses transporter proteins such as the P-glycoprotein (P-gp). The BBEC cells are grown, in the presence of astrocytes, on a filter where they form tight junctions between themselves. The peptide is then added to the apical compartment. Samples from both the apical and basal compartments, which represent the blood and brain, respectively, are taken at different times and analysed by HPLC.

As described by Artursson [49], the apparent permeability coefficient can be calculated according to the formula $P_{app} = (dQ/dt)/(A \cdot C_0)$, where dQ/dt represents the amount of compound transported per second ($\mu\text{mol/s}$), A is the surface area of the filter (cm^2) and C_0 is the initial concentration of compound ($\mu\text{mol/ml}$).

In order to adapt this model assay to a high throughput method, the experimental design of the transport study has been simplified by calculating only the percentage of transport after a fixed period of time (60 min), known as $\%T_{3600}$, instead of calculating the P_{app} . It should be noted that the $\%T_{3600}$ shows a good linearity with the P_{app} values [50]. This simplification allows the reduction of the total number of samples to be analysed by HPLC and also eliminates the need for the manipulation of plates during the study. In order to normalize the values, the $\%T_{3600}$ of each compound was calculated and was referred to the $\%T_{3600}$ of a reference compound (propranolol) transported across the BBB [51].

Four different peptides previously reported to be capable of crossing the BBB [52–54] (see experimental section) were used to optimize different parameters of the *in vitro* assay, including initial concentration, transwell surface size and time of analysis.

Once the *in vitro* assay was optimized, the first generation of peptides was evaluated with the *in vitro* cell-based assay, providing the $\%T_{3600}$ values shown in Table 3A.

After collecting the data from the exploration of these four techniques ($\log P_{\text{octanol/water}}$, HPLC RP-C₁₈, IAMC and BBEC), four different rankings were built for the first generation of peptides (Table 3).

In the cell-based assay (BBEC), several transport mechanisms are involved, while for the other techniques only passive diffusion is involved.

The peptides can be grouped into three classes based on the degree to which they were transported in the cell-based assay (Table 3A): a well transported class, a

moderately transported class and a poorly transported class.

Peptides that were well transported by BBEC varied greatly in rankings for the other methods studied, which only predict passive diffusion. However, peptide 3 was predicted by all techniques to effectively cross the BBB. This observation thus led to the hypothesis that peptide 3 crosses the BBB by passive diffusion.

In the case of peptide 22, a mechanism different from passive diffusion may be involved. Further studies need to be done to establish the transport mechanisms for peptides 3 and 22 (Figure 9), but a surprising initial conclusion is that the presence of residues with charged side-chains does not prevent their passage across the barrier. It seems also important to reduce the ability of the peptide backbone to form hydrogen bonds. In spite of the synthetic challenges associated with the introduction of *N*-methyl amino acids, their use offers a direct way to eliminate hydrogen bond formation.

Taking into account those cases where peptides were not well transported, it can be seen that only IAMC predicted the same results as the cell-based assay.

In selecting one technique as an evaluative tool for this field, one must consider the transport mechanism to be studied, the amenability of the technique to high throughput, and the tendency of the technique to generate false-positives. For all the aforementioned reasons, IAMC appears to be a convenient tool.

Creation of the Second Generation

Based upon the ranking obtained for the first generation by IAMC, the genetic algorithm has generated the second generation of chromosomes (Figure 10).

The genetic algorithm chose the parents of the second generation by fitness ranking and subsequently mated them. One-point random cross-overs were then used to obtain the children.

Finally, random mutations to all possible alleles took place, thereby yielding a new group of chromosomes. In addition to these new chromosomes, the new generation contained the best chromosomes from the previous generation (elitism). At this point, peptides needed to be selected for each chromosome, synthesized and evaluated.

CONCLUSIONS

A highly integrated approach using evolutionary computational tools, solid-phase peptide synthesis and an HPLC-based BBB model has led to a collection of medium-sized peptides among which were found several with interesting BBB-transport properties. This finding is very promising for the course of the entire project as the first generation was only generated randomly (no evolution applied yet). Analysis of the structural features of the best candidates show that

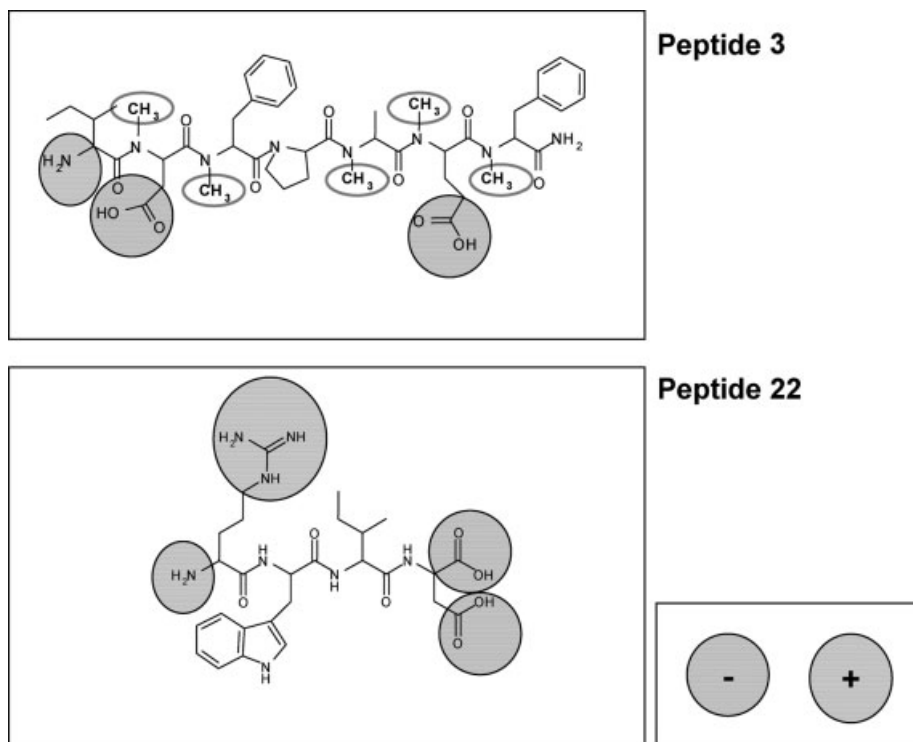


Figure 9 Structures of peptide 3 and peptide 22.

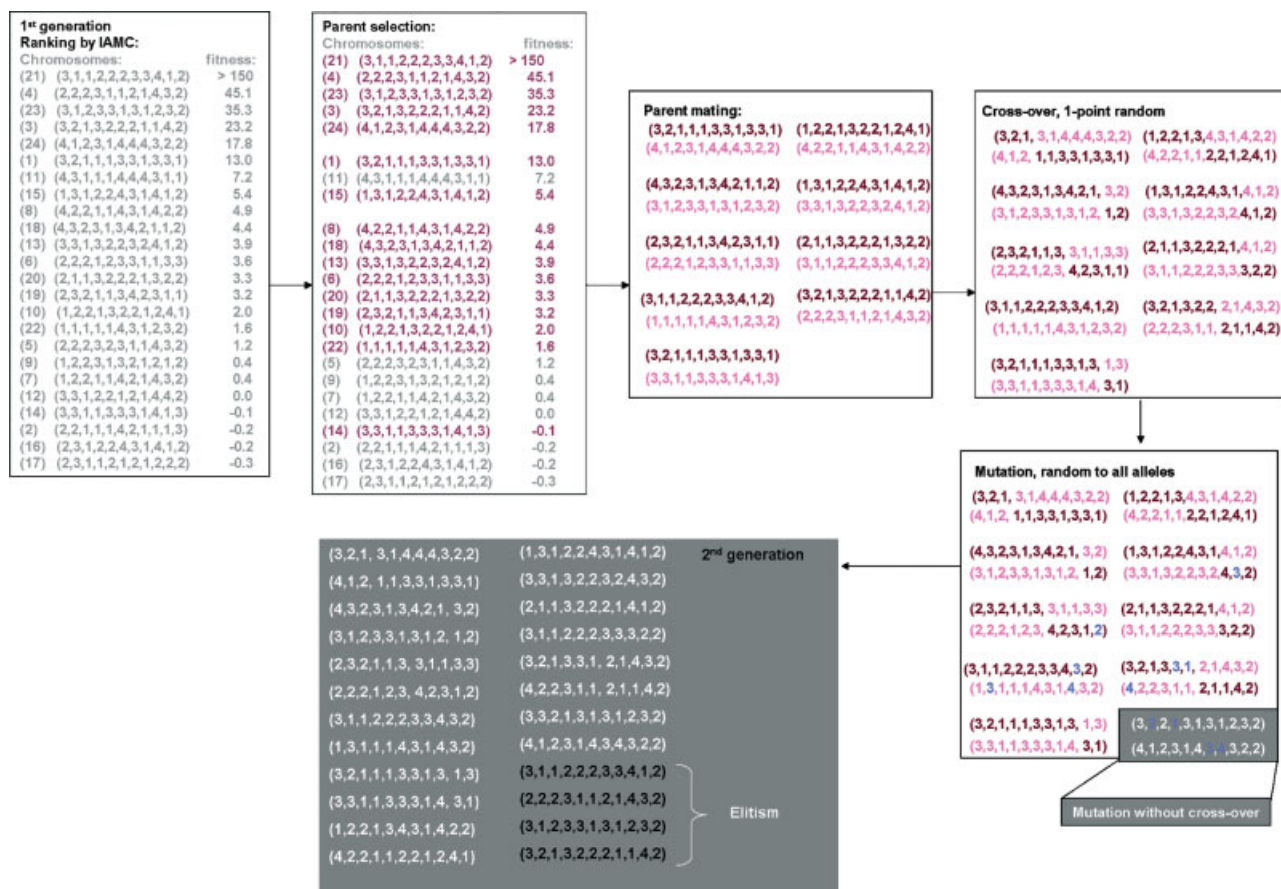


Figure 10 Creation of the chromosomes of the second generation based on the ranking obtained for the first generation.

their properties could hardly have been anticipated by application of the standard rules normally used for predicting ADME properties of small organic molecules. Further application of this combined approach will pave the way to the discovery of new peptides with even better BBB-transport properties.

MATERIALS AND GENERAL METHODS

Materials and Equipment

Protected amino acids were obtained from Luxembourg Industries (Tel-Aviv, Israel), Neosystem (Strasbourg, France), Calbiochem-Novabiochem AG (Laüfelfingen, Switzerland) and Bachem AG (Bubendorf, Switzerland). PyBOP, Fmoc-AM handle, and solid supports were supplied by Calbiochem-Novabiochem AG. Barlos resin was kindly donated by Rohm & Haas (Spring House, PA). DIPCI was obtained from Fluka Chemika (Buchs, Switzerland), TBTU and HOBt from Albatros Chem. Inc. (Montreal, Canada). PyAOP was supplied Applied Biosystems, HOAt from GL Biochem Shanghai and HATU was supplied from Applied Biosystems. Solvents for peptide synthesis and RP-HPLC were obtained from Scharlau (Barcelona, Spain). Trifluoroacetic acid was supplied by KaliChemie (Bad Wimpfen, Germany). Other chemicals used were obtained from Aldrich (Milwaukee, WI) and were of the highest purity commercially available. All commercial reagents and solvents were used as received, with the exception of DCM and DMF. DMF was bubbled with nitrogen to remove volatile contaminants and stored over activated 4 Å molecular sieves (Merck, Darmstadt, Germany). DCM was passed through a short column of Al₂O₃ (in the case of DCM used for peptide synthesis). HPLC was performed using a Waters Alliance 2695 (Waters, Massachusetts, USA) chromatography system with a PDA 995 detector, a reverse-phase Symmetry C₁₈ (4.6 × 150 mm) 5 µm column, and H₂O with 0.045% TFA and MeCN with 0.036% TFA as mobile phases. IAM column (10 × 4.6 mm, 12 µm, 300 Å, IAM.PC.DD2 column, Regis Technologies Inc., Morton Grove, Illinois, USA). Mass spectra were recorded on a MALDI Voyager DE RP time-of-flight (TOF) spectrometer (PE Biosystems, Foster City, CA, USA). Peptide resin samples were hydrolysed in 12 N aqueous HCl/propionic acid (1 : 1 v/v) at 155 °C for 1–3 h. Subsequent amino acid analyses were performed on a Beckman System 6300 autoanalyser (Fullerton, California, USA).

Transwell filter inserts were from Cultek (Madrid, Spain). DMEM medium, horse serum, newborn calf serum and fetal calf serum were obtained from Life-Technologies-Gibco (Maryland, USA). Glutamine, gentamicine, rat tail type I collagen, basic fibroblast growth factor and HBSS buffer were from Sigma. TEER volt-ohmmeter from World Precision Instruments Inc. (Hertfordshire, UK). Radioactive products [³H]-inuline and DL-[4-³H]-propranolol, were from Amersham Pharmacia Biotech (Buckinghamshire, UK).

General Procedures

Peptide elongation and other manipulations on solid phase were carried out in polypropylene syringes fitted with a polyethylene porous disk. Solvents and soluble reagents were removed by suction. Washings between deprotection, coupling

and subsequent deprotection steps were carried out with DMF (5 × 0.5 min) and DCM (5 × 0.5 min) using 10 ml of solvent/g of resin for each wash. Syntheses of C-terminal amide peptides were carried out with 100 µmol of Fmoc-AM-*p*-MBHA resin (0.3 mmol/g). In the case of C-terminal acid peptides and for the precursors of *N*-methyl amide peptides, Barlos resin was used (nominal loading, 1.5 mmol/g) and the loading was reduced to 0.75–0.90 mmol/g after partial incorporation of the first Fmoc-amino acid. Syntheses were carried out on a 100 µmol scale.

Manual Removal of the Fmoc Protecting Group

Fmoc groups were removed with two treatments of 10 min with piperidine/DMF (2 : 8, v/v). Two extra treatments of 5 min with piperidine/DBU/toluene/DMF (5 : 5 : 20 : 70, v/v) were used for the *N*-methyl amino residues.

Coupling Methods

Methods 1 and 2 were used for couplings to non-*N*-methyl amino acids. Methods 3, 4, 5 and 6 were used for couplings to *N*-methyl amino acids.

Method 1. Protected amino acid (4 equiv.) in DMF (1–3 ml/g resin), TBTU (4 equiv.) and DIEA (8 equiv.) were sequentially added to the resin and the mixture was allowed to react with intermittent manual stirring for 1 h.

Method 2. Protected amino acid (4 equiv.) and HOBt (4 equiv.) in DCM (1–3 ml/g resin) and DIPCI (4 equiv.) were sequentially added to the resin and the mixture was allowed to react for 1 h with intermittent manual stirring.

Method 3. Protected amino acid (4 equiv.) and HOAt (12 equiv.) in DMF (1–3 ml/g resin), PyBOP (4 equiv.) and DIEA (12 equiv.) were sequentially added to the resin and the mixture was allowed to react for 90 min with intermittent manual stirring.

Method 4. Protected amino acid (5 equiv.) in DMF (1–3 ml/g resin), HATU (5 equiv.) and DIEA (10 equiv.) were sequentially added to the resin and allowed to react with intermittent manual stirring for 30 min.

Method 5. Protected amino acid (5 equiv.) in DMF (1–3 ml/g resin), PyAOP (5 equiv.) and DIEA (10 equiv.) were sequentially added to the resin and allowed to react with intermittent manual stirring for 1 h. PyAOP (2.5 equiv.) was then added and the mixture was allowed to react for an additional 60 min.

Method 6. Protected amino acid (4 equiv.) in DCM/DMF (1 : 1, v/v) (1–3 ml/g resin) and DIPCI (2 equiv.) were used to prepare the symmetric anhydride. The resulting urea was eliminated by filtration, the solution was added to the resin and the mixture was allowed to react with intermittent manual stirring for 1 h.

Anchoring of the first amino acid to the Barlos resin was achieved by taking the Fmoc-amino acid (0.5 equiv.) and DIEA (5 equiv.) up in DCM and stirring the resulting slurry for 1 h. The unreacted Cl groups were capped by addition of

MeOH (1 ml/g resin) and, after removal of the Fmoc group, the loading was calculated by amino acid analysis of a hydrolysed sample.

Acetylation of *N*-terminal Function

Depending on the peptide sequence, acetylation was performed on solid-phase or in solution. On solid-phase, a standard protocol of Ac₂O (50 equiv.) and DIEA (50 equiv.) in DMF for 20 min was used. Various conditions were tested for acetylation in solution.

- (A) Ac₂O (5 mmol) and DIEA (5 mmol) in DMF for 90 min.
- (B) AcOH (4 equiv.) and DIPCI (4 equiv.) in DCM for 2 h.
- (C) Ac₂O (2 equiv.) and DIEA (2 equiv.) in DMF for 5 min.

The acetylation products were confirmed by MALDI-TOF spectrometry.

Cleavage of the Peptides

Final unprotected amide or free carboxylic peptides were cleaved from the resin with one of the following cleavage cocktails: TFA/H₂O/EDT-*i*Pr₃SiH (94.5:2.5:2:1, v/v), TFA/H₂O/*i*Pr₃SiH (95:2.5:2.5, v/v), or TFA/H₂O/EDT/*i*Pr₃SiH/thioanisole/phenol (81.5:5:2.5:1:5:5 v/v), depending on the peptide sequence, for 60–90 min (10 ml/g resin). Peptides were precipitated by addition of cold MTBE, the solution was decanted and the solid was triturated with cold MTBE, which was again decanted. The process was repeated twice.

Cleavages of partially protected peptides to be amidated in solution to form the *C*-terminal *N*-methyl amide were obtained from the Barlos resin with TFA/DCM (2:98, v/v) (3 × 3 min) (10 ml/g resin). The filtrates were collected over pyridine/DCM (1:99, v/v) (50 ml/g resin) and the combined solutions were evaporated to dryness under reduced pressure and lyophilized.

The procedure used for removal of the side chain protecting groups in solution was similar to that used for solid-phase.

Amidation of *C*-terminal Free Carboxylic Acids in Solution

Peptides without lateral groups susceptible to amidation were used in their unprotected form. Amidation was performed in solution by dissolving the peptides in anhydrous DMF. HOBt (1.5 equiv.) was dispersed in 10 ml of water using a sonicating bath. While maintaining the dispersion, 40% aqueous CH₃NH₂ (1.5 equiv.) was added. The mixture was kept in the sonicating bath for 5 min at room temperature and the solution was then lyophilized. Methylamine salt of HOBt (3.0 equiv.) and DIPCI (2.2 equiv.) were added at a concentration of 25 mg/ml and allowed to react at 47 °C for 7–10 h. The reaction was monitored by MALDI-TOF spectrometry.

Peptide Purification

Purification of the crude peptides was performed by semipreparative HPLC (Waters Controller 600 and Fraction Collector II, Simple Manager 2700 autoinjector, and a 2487 UV/VIS detector). The column used was a 5 μm Symmetry C₁₈ (30 × 100 mm) with a flow rate of 10 ml/min. The mobile

phases used were H₂O with 0.1% TFA and MeCN with 0.1% TFA.

Peptide Characterization and Quantification

Peptide purity was calculated by HPLC RP-C₁₈ and the peptide identity confirmed by MALDI-TOF spectrometry and amino acid analysis. Peptides were quantified by amino acid analysis on a Beckman System 6300 autoanalyser after being hydrolysed in aqueous HCl 6 N 1% phenol at 155 °C for 1–3 h.

Synthesis of Control Peptides

(A) RC-161: Ac-*D*-Phe-Cys-Tyr-*D*-Trp-Lys-Val-Cys-Thr-NH₂.

This peptide was synthesized following a Boc/Bzl protecting scheme. Starting with 143 mg of *p*-MBHA resin (0.7 mmol/g) the elongation was carried out using TBTU with *in situ* neutralization as the coupling method. After the elongation and *N*-terminal Boc deprotection, *N*-terminal acetylation was carried out using 5 mmol Ac₂O (476 μl) and 5 mmol of DIEA (850 μl) in DMF for 30 min. The progress of couplings and acetylations was monitored by the ninhydrin test [55].

Subsequent elimination of the formyl protecting group was achieved with two treatments of 10 min each with piperidine 50% in DMF.

Finally, the resin was washed with MeOH and dried by suction. Peptide cleavage from the resin and lateral chain deprotection was accomplished using HF_{anh}/anisole (9:1, v/v, 5 ml) for 1 h at 0 °C. The crude product from the acidolysis was analysed by HPLC RP-C₁₈ and MALDI-TOF [M + H]⁺: 1090.87 Da.

The disulfur bridge formation was done by oxidation at high dilution (50 μM) of the linear precursor in solution, in 10 mM NH₄HCO₃ buffer at pH 8. The cyclization process was checked by HPLC, MALDI-TOF and Ellman test at different times [56]. The cyclization was completed after 96 h. The reaction was stopped by acidifying the mixture with AcOH. The solvent was evaporated to dryness under reduced pressure and lyophilized. Global yield: 25.1%. Purity: > 90%, MALDI-TOF, [M + H]⁺: 1088.93 Da, AAA: Thr 1.03 (1), Val 0.64 (1), Tyr 0.73 (1), Phe 0.97 (1), Lys 1.28 (1)

(B) AVP 1-9: H-Cys-Tyr-Phe-Gln-Asn-Cys-Pro-Lys-Gly-NH₂.

This peptide was synthesized following the Fmoc/Bu^t protecting scheme. The *p*-MBHA resin (143 mg, 0.7 mmol/g) was functionalized with Fmoc-AM linker (5 equiv.) using TBTU in DMF for 16 h. The extent of the couplings was checked by the ninhydrin test [55].

After the peptide elongation using TBTU as the coupling reagent, *N*-terminal Fmoc groups were removed. Finally, the resin was washed with MeOH and dried by suction. Peptide cleavage from the resin and lateral chain deprotection was accomplished using TFA/thioanisole/EDT/anisole (90:5:3:2, v/v) for 1 h. The crude product from the acidolysis crude was analysed by HPLC and MALDI-TOF [M + H]⁺: 1059.32 Da.

The linear precursor was purified using an HPLC-prep before the cyclization step: 5%–40% MeCN in H₂O for 40 min.

Disulfide bridges were formed by oxidation of the pure linear precursor in solution at high dilution (50 μM), in 10 mM NH₄HCO₃ buffer at pH 8. The cyclization process was checked by HPLC, MALDI-TOF and the Ellman test at different times

[56]. The cyclization was completed after 1 h. The reaction was quenched by acidifying the mixture with AcOH. The solvent was evaporated to dryness under reduced pressure and lyophilized. Global yield: 21.2%. Purity: > 90%, MALDI-TOF, $[M + H]^+$: 1057.30 Da, AAA: Asx 0.95 (1), Glx 0.86 (1), Gly 1.09 (1), Tyr 0.80 (1), Phe 0.93 (1), Lys 1.36 (1), Pro 0.94 (1).

(C) Met⁵-Enk: H-Tyr-Gly-Gly-Phe-Met-OH. This peptide was synthesized following a Fmoc/Bu^t protecting scheme. Starting with 143 mg of *p*-MBHA resin (0.7 mmol/g), the resin was functionalized with AB linker (5 equiv.) using TBTU in DMF for 16 h. The first amino acid was introduced using 4 equiv. of the corresponding protected amino acid, 4 equiv. DIPCI and 0.4 equiv DMAP (2 × 30 min). This incorporation was checked by an hydroxyl test [57]. The elongation was carried out using TBTU as the coupling reagent. The couplings were monitored by the ninhydrin test [55].

Subsequently Fmoc protecting groups were removed. Finally, the resin was washed with MeOH, dried by suction and cleaved from the resin. Side chain deprotection and cleavage were accomplished using TFA/thioanisole/EDT/anisole (90:5:3:2, v/v) for 1 h. The crude product from the acidolysis was analysed by HPLC and MALDI-TOF $[M + H]^+$: 574.80 Da, global yield: 47.4%, purity: > 95%, AAA: Gly 2.17 (2), Met 0.82 (1), Tyr 0.92 (1), Phe 0.91 (1).

(D) Ac-MePhe-MePhe-MePhe-NH₂. The peptide was synthesized following a Fmoc/Bu^t protecting scheme. Starting with 151 mg of Fmoc-AM-*p*-MBHA resin (0.66 mmol/g), the first amino acid was incorporated using TBTU as the coupling reagent. This incorporation was checked by the ninhydrin test [55]. The elongation was continued using protected amino acids (4 equiv.) and HOAt (12 equiv.) in DMF (1–3 ml/g resin) followed by PyBOP (4 equiv.) and DIEA (12 equiv.) with intermittent manual stirring for 90 min. Subsequent couplings were checked by the De Clercq test [58]. Fmoc deprotection was carried out by two treatments of 10 min with piperidine/DMF (2:8, v/v) and two extra treatments of 5 min with piperidine/DBU/toluene/DMF (5:5:20:70, v/v).

After elongation, the Fmoc group was removed followed by cleavage of the peptide from the resin. Side chain deprotection and cleavage were accomplished using TFA/H₂O (95:5, v/v) for 1 h. The crude product from the acidolysis was analysed by HPLC and MALDI-TOF $[M + H]^+$: 501.25 Da.

Acetylation was performed in solution using Ac₂O (5 mmol, 476 µl) and DIEA (5 mmol, 850 µl) in DMF for 60 min.

The acetylation products were confirmed by MALDI-TOF spectrometry, 543.2 Da. Global yield: 91.2%, purity: >90%.

Log *P*_{octanol/water}

The log *P*_{octanol/water} values for the peptides of the first generation were calculated using the PLOGP program. PLOGP program was downloaded for free from (ftp2.ipc.pku.edu.cn), 'pub/software/plogp'.

IAMC

Peptide retention times were determined using an IAM column (10 × 4.6 mm, 12 µm, 300 Å, IAM.PC.DD2 column, Regis Technologies Inc., Morton Grove, Illinois, USA). For all tested

compounds, the injection volume was 20 µl of a solute aqueous solution (100 µg/ml). IAM chromatography was carried out isocratically using a 10 mM phosphate buffer, 2.7 mM KCl and 137 mM NaCl solution at pH 7.4 with a flow rate of 1 ml/min. Compounds were detected by UV absorption at 220 nm.

The retention times *t_r* and *t₀* correspond to the compound being studied and a marker compound of the column dead time/void volume (citric acid), respectively.

HPLC RP-C₁₈

Peptide retention times by RP-HPLC were determined using a Symmetry C₁₈ column (150 × 4.6 mm, 5 µm, 100 Å) in a linear gradient of 0–100% MeCN (+0.036% TFA) in H₂O (+0.045% TFA) over 15 min at a flow rate of 1 ml/min and UV detection at 220 nm. For all compounds, the injection volume was 20 µl of a solute aqueous solution (100 µg/ml).

BBEC Assay

Cell culture. Fresh bovine brains were obtained from a local slaughterhouse (Mercabarna, Barcelona) under veterinary supervision. Bovine brain endothelial cells were isolated from brain grey matter by mechanical methods and were seeded at 50 000 cells/cm² onto 24 mm diameter Transwell filter inserts with 0.4 µm pores coated with rat tail type I collagen (20 µg/ml). Cells were grown in DMEM, 10% horse serum, 10% newborn calf serum, 2 mM glutamine, 0.5 µg/ml gentamicine and basic fibroblast growth factor (1 ng/ml).

Astrocytes were isolated from newborn rat cerebral cortex. Briefly, animals were killed by spinal dislocation and after removing the meninges, brain tissue was forced gently through an 82 µm nylon sieve. Astrocytes were plated on a 6-well microplate in 2 ml of DMEM supplemented with 10% fetal calf serum. The *in vitro* model of bovine BBB used in this study was obtained by co-culturing BBEC at 40 000 cells/cm² onto 24 mm diameter Transwell filter inserts with 0.4 µm pores coated with rat tail type I collagen (20 µg/ml) with astrocytes in the lower compartment. Under these conditions, BBEC differentiate after 12 days into a confluent polarized monolayer that closely mimics *in vivo* the BBB. To control the BBB status of BBEC polarized cultures, transendothelial electrical resistance (TEER) and paracellular permeability were checked. The experiments were approved by the ethical committee of the University of Barcelona.

Transendothelial transport study. Once the BBB model was formed, BBEC-seeded supports were transferred to new receiving wells to avoid any interference from the astrocyte population. Cells were washed carefully with Hank's balanced salt solution (HBSS) buffer (KCl 540 µM; KH₂PO₄ 44 µM; NaCl 13.68 mM; NaHPO₄ 33 µM; CaCl₂ 1.3 mM; MgCl₂ 1.1 mM). The peptides were added to the upper compartment 1.5 ml (initial concentration, 1 mM in HBSS buffer) and the basal compartment was then filled with 3 ml HBSS buffer. The transwell plate was maintained at 37 °C in a humidified atmosphere. Samples (150 µl) were taken from each compartment at time points (0 and 60 min) and frozen at –80 °C until analysing them by HPLC RP-C₁₈ with UV detection. [³H]-inuline and DL-[4-³H]-propranolol were applied apically as negative and positive controls for passive diffusion. The apparent permeability coefficient was calculated according to the formula

$P_{app} = (dQ/dt)/(A \cdot C_0)$, as described by Artursson [49], in which dQ/dt represents the amount of compound transported per second ($\mu\text{mol/s}$), A is the surface area of the filter (cm^2) and C_0 is the initial concentration of compound ($\mu\text{mol/ml}$). For peptides 10 and 17, 0.5% DMSO was added to the apical and basal compartments to ensure solubility. Corresponding controls using [^3H]-inuline and DL-[4- ^3H]-propranolol with 0.5% DMSO were performed in parallel.

In order to adapt this model assay to a high throughput method, the percentage of transport after 60 min, ($\%T_{3600}$), was calculated instead of the P_{app} values. This parameter shows a good linearity with the P_{app} values [50]. In order to normalize the values, the $\%T_{3600}$ of each compound was referred to the $\%T_{3600}$ of propranolol.

Genetic Algorithm

The evolutionary algorithm used is a Simple Genetic Algorithm (SGA) [59]. Some SGA parameters were optimized using a genetic metaalgorithm [28]. The parameters were the following: genetic algorithm geometry (24 peptides \times 10 generations), percentage of replication (20%), cross-over probability (0.95) and mutation probability (0.1). The rest of genetic algorithm parameters were set taking into account the scenery where SGA was going to work. These parameters were the following: uniform random initialization, stochastic universal sampling, one-point cross-over and uniform mutation.

Acknowledgements

The authors thank Dr X. Roselló for fruitful discussions during the realization of this study and Ms S. González and Ms E. Rodríguez-Millán for their excellent technical assistance. This work was supported by Generalitat de Catalunya [CeRBA and Grups Consolidats (2001 SGR 00047)], Ministerio de Ciencia y Tecnología (BIO 2002-02301, EET2001-4813 and BQU 2003-00089) and Fundació La Marató TV3-2002 ref. 013010.

REFERENCES

- Marx J. NGF and Alzheimer's: hopes and fears. *Science* 1990; **247**: 408–410.
- Scheld WM. Drug delivery to the central nervous system: General principles and relevance to therapy for infections of the central nervous system. *Rev. Infect. Dis.* 1989; **11**: S1669–S1690.
- Ehrlich P. *Das Sauerstoffbedürfnis des Organismus; Eine Farbenanalytische Studie*. 1885; Berlin, Hirschwald.
- Goldmann EE. Die aussere und innere Sekretion des gesunden und kranken Organismus im Lichte der vitalen Färbung. *Beitr. Klin. Chir.* 1909; **64**: 192–265.
- Reese TS, Karnovsky MJ. Fine structural localization of a blood–brain barrier to exogenous peroxidase. *J. Cell Biol.* 1967; **34**: 207–217.
- Brightmann MW, Reese TS, Feder N. Assessment with the electron-microscope of the permeability to peroxidase of cerebral endothelium and epithelium in mice and sharks. In *Capillary Permeability*, Crone C, Lassen NA (eds). Munksgaard: Copenhagen, 1970; 463.
- Lipinski CA, Lombardo F, Dominy BW, Feeney PJ. Experimental and computational approaches to estimate solubility and permeability in drug discovery and development settings. *Adv. Drug Deliv. Rev.* 1997; **23**: 3–25.
- Norinder U, Haeberlein M. Computational approaches to the prediction of blood–brain barrier distribution. *Adv. Drug Deliv. Rev.* 2002; **54**: 291–313.
- Van de Waterbeemd H, Camenisch G, Folkers G, Chretien JR, Raevsky OA. Estimation of blood–brain barrier crossing of drugs using molecular size and shape, and H-bonding descriptors. *J. Drug Targeting* 1998; **6**: 151–165.
- Kelder J, Grootenhuis PD, Bayada DM, Delbressine LP, Ploemen JP. Polar molecular surface area as a dominating determinant for oral absorption and brain permeation of drugs. *Pharm. Res.* 1999; **16**: 1514–1519.
- Doan KMM, Humpreys JE, Webster LO, Wring SA, Shampire LJ, Serabjit-Singh CJ, Adkinson KK, Polli JW. Passive permeability and P-glycoprotein-mediated efflux differentiate central nervous system (CNS) and non-CNS marketed drugs. *J. Pharmacol. Exp. Ther.* 2002; **303**: 1029–1037.
- Kastin AJ, Nissen C, Nikolics K, Meedzihradsky K, Coy DH, Teplan I, Schally AV. Distribution of ^3H - α -MSH in rat brain. *Brain Res. Bull.* 1976; **1**: 19–26.
- Kastin AJ, Olson RD, Schally AV, Coy DH. CNS effects of peripherally administered brain peptides. *Life Sci.* 1979; **25**: 401–414.
- Gray RA, Van der Velde DG, Burke CJ, Manning MC, Middaugh CR, Borchardt RT. Delta-sleep-inducing peptide: Solution conformational studies of a membrane-permeable peptide. *Biochemistry* 1994; **33**: 1323–1331.
- Burton PS, Conradi RA, Ho NFH, Hilgers AR, Borchardt RT. How structural features influence the biomembrane permeability of peptides. *J. Pharm. Sci.* 1996; **85**: 1336–1340.
- Holland JH. *Adaptation in Natural and Artificial Systems*. The University of Michigan Press: Ann Arbor, 1975.
- Cecchelli R, Dehouck B, Descamps L, Fénart L, Buée-Scherrer V, Lundquist S, Rentfel M, Torpier T, Dehouck MP. *In vitro* model for evaluating drug transport across the blood–brain barrier. *Adv. Drug Deliv. Rev.* 1999; **36**: 165–178.
- Levin LA. Relationship of octanol-water partition coefficient and molecular weight to rat brain capillary permeability. *J. Med. Chem.* 1980; **23**: 682–684.
- Bernards MD, Hill HF. Physical and chemical properties of drug molecules governing their diffusion through the spinal meninges. *Anesthesiology* 1992; **77**: 750–756.
- Macheras PE, Symillides MY. Towards a quantitative approach for the prediction of the fraction of dose absorbed using the absorption potential concept. *Biopharm. Drug. Dispos.* 1989; **10**: 43–53.
- Nook T, Doelker E, Buri P. Intestinal absorption kinetics of various model drugs in relation to partition coefficients. *Int. J. Pharm.* 1988; **43**: 119–129.
- Komiya I, Park JY, Kamani A, Ho NFH, Higuchi WI. Quantitative mechanistic studies in simultaneous fluid flow and intestinal absorption using steroids as model solutes. *Int. J. Pharm.* 1980; **4**: 249–262.
- Ho NFH, Park JY, Morozowich W, Higuchi WI. In *Design of Biopharmaceutical Properties through Prodrugs and Analogs*, Roche EB (ed.). American Pharmaceutical Association, Academy of Pharmaceutical Science. Washington, DC. 1977; 136–227.
- Van Bree JBMM, De Boer AG, Danhof M, Ginsel LA, Breimer DD. Characterisation of an *in vitro* blood–brain barrier: effects of molecular size and lipophilicity on cerebrovascular endothelial transport rates of drugs. *J. Pharmacol. Exp. Ther.* 1988; **247**: 1233–1239.
- Tavakoli-Saberi MR, Audus KL. Physicochemical factors affecting β -adrenergic antagonist permeation across cultured hamster pouch buccal epithelium. *Int. J. Pharm.* 1989; **56**: 135–142.
- Pardridge WM. *Peptide Drug Delivery to the Brain*. Raven Press: New York, 1991; 1–357.
- Kaiser ET, Kadzy FJ. Peptides with affinity for membranes. *Ann. Rev. Biophys. Chem.* 1987; **16**: 561–581.

28. Teixidó M, Belda I, Roselló X, González S, Fabre M, Llorà X, Bacardit J, Garrell JM, Vilaró S, Albericio F, Giralt E. Development of a genetic algorithm to design and identify peptides that can cross the blood–brain barrier. 1. Design and validation *in silico*. *QSAR Comb. Sci.* 2003; **22**: 745–753.
29. Teixidó M, Albericio F, Giralt E. Solid-phase synthesis and characterization of *N*-methyl rich peptides. *J. Pept. Res.* 2005; **65**: 153–166.
30. Falb E, Yechezkel T, Salitra Y, Gilon C. *In situ* generation of Fmoc-amino acid chlorides using bis-(trichloromethyl)carbonate and its utilization for difficult couplings in solid-phase peptide synthesis. *J. Pept. Res.* 1999; **53**: 507–517.
31. Merrifield RB, Mitchell AR, Clarke JE. Detection and prevention of urethane acylation during solid-phase peptide synthesis by anhydride methods. *J. Org. Chem.* 1974; **39**: 660–668.
32. Merrifield RB, Singer J, Chait BT. Mass spectrometric evaluation of synthetic peptides for deletions and insertions. *Anal. Biochem.* 1988; **174**: 399–414.
33. Urban J, Vaisar T, Shen R, Lee MS. Lability of *N*-alkylated peptides towards TFA cleavage. *Int. J. Pept. Prot. Res.* 1996; **47**: 182–189.
34. Juhler M. Simultaneous determination of regional cerebral blood flow, glucose metabolism, and pH in acute experimental allergic encephalomyelitis. *J. Cerebr. Blood Flow Metab.* 1987; **7**: 578–584.
35. De Boer AG, De Vries HE, De Lange ECM, Danhof M, Kuiper J, Breimer DD. Drug transport to the brain: *in vitro* versus *in vivo* approaches. *J. Contr. Rel.* 1994; **28**: 259–263.
36. Benveniste H, Huttermeier PC. Microdialysis: Theory and applications. *Progress Neurobiol.* 1990; **35**: 195–215.
37. Meyer HH. Zur Theorie der Alkoholnarkose. *Arch. Exp. Pathol. Pharmacol.* 1899; **42**: 109–118.
38. Overton E. *Studien Über Die Narkose*. Fischer Verlag: Jena, Germany, 1901.
39. Rogers JA, Wong A. The temperature dependence and thermodynamics of partitioning of phenols in the *n*-octanol–water system *Int. J. Pharm.* 1980; **6**: 339–348.
40. Tao P, Wang R, Lai L. Calculating partition coefficients of peptides by the addition method. *J. Mol. Model.* 1999; **5**: 189–195.
41. Katz Y, Diamond J M. A method for measuring nonelectrolyte partition coefficient between liposomes and water. *J. Membr. Biol.* 1974; **17**: 69–86.
42. Betageri GV, Rogers JA. Thermodynamics of partitioning of β -blockers in the *n*-octanol–buffer and liposome systems. *Int. J. Pharm.* 1987; **36**: 165–173.
43. Reig F, Busquets MA, Haro I, Rabanal F, Alsina MA. Interaction of opiate molecules with lipid monolayers and liposomes. *J. Pharm. Sci.* 1992; **81**: 546–550.
44. Pidgeon C, Venkataran UV. Immobilized artificial membrane chromatography: supports composed of membrane lipids. *Anal. Biochem.* 1989; **176**: 36–47.
45. Pidgeon C, Stevens J, Otto S, Jefcoate C, Marcus C. Immobilized artificial membrane chromatography: rapid purification of functional membrane proteins. *Anal. Biochem.* 1991; **194**: 163–173.
46. Chui WK, Wainer I. Enzyme-based high-performance liquid chromatography supports as probes of enzyme activity and inhibition: the immobilization of trypsin and α -chymotrypsin on an immobilized artificial membrane high-performance liquid chromatography support. *Anal. Biochem.* 1992; **201**: 237–245.
47. Braddy AC, Janaky T, Prokai L. Immobilized artificial membrane chromatography coupled with atmospheric pressure ionization mass spectrometry. *J. Chrom. A* 2002; **966**: 81–87.
48. Pidgeon C, Ong S, Liu H, Qiu X, Pidgeon M, Dantzig AH, Munroe J, Hornback WJ, Kasher JS. IAM chromatography: an *in vitro* screen for predicting drug membrane permeability. *J. Med. Chem.* 1995; **38**: 590–594.
49. Artursson P, Karlsson J. Correlation between oral drug absorption in humans and apparent drug permeability coefficients in human intestinal epithelial (Caco-2) cells. *Biochem. Biophys. Res. Commun.* 1991; **175**: 880–885.
50. Otis KW, Avery ML, Broward-Partin SM, Hansen DK, Behlow HW, Scott DO, Thompson TN. Evaluation of the BBMEC model for screening the CNS permeability of drugs. *J. Pharmacol. Toxicol. Meth.* 2001; **45**: 71–77.
51. Dehouck MP, Dehouck B, Schluep C, Lemaire M, Cecchelli R. Drug transport to the brain: comparison between *in vitro* and *in vivo* models of the blood–brain barrier. *Eur. J. Pharm. Sci.* 1995; **3**: 357–365.
52. Banks WA, Schally AV, Barrera CM, Fasold MB, Durham DA, Csernus VJ, Groot K, Kastin AJ. Permeability of the murine blood–brain barrier to some octapeptide analogs of somatostatin. *Proc. Natl Acad. Sci. USA* 1990; **87**: 6762–6766.
53. Van Bree JBMM, De Boer AG, Verhoef JC, Danhof M, Breimer DD. Transport of vasopressin fragments across the blood–brain barrier: *in vitro* studies using monolayer cultures of bovine brain endothelial cells. *J. Pharm. Exp. Ther.* 1989; **249**: 901–905.
54. Weber SJ, Abbruscato TJ, Brownson EA, Lipkowski AW, Polt R, Misicka A, Haaseth RC, Bartosz H, Hraby VJ, Davis TP. Assessment of an *in vitro* blood–brain barrier model using several [Met⁵]enkephalin opioid analogs. *J. Pharm. Exp. Ther.* 1993; **266**: 1649–1655.
55. Kaiser E, Colescott RL, Bossinger CD, Cook PI. Color test for detection of free terminal amino groups in solid-phase synthesis of peptides. *Anal. Biochem.* 1970; **34**: 595–598.
56. Ellman GM. Tissue sulfhydryl groups. *Arch. Biochem. Biophys.* 1959; **82**: 70–77.
57. Kuisle O, Lolo M, Quiñoa E, Riguera R. Monitoring the solid-phase synthesis of depsides and depsipeptides. A color test for hydroxyl groups linked to a resin. *Tetrahedron* 1999; **55**: 14 807–14 812.
58. Maddar A, Farcy N, Hosten NGC, De Muynck H, De Clercq PJ, Barry J, Davis AP. A novel sensitive colorimetric assay for visual detection of solid-phase-bound amines. *Eur. J. Org. Chem.* 1999; **11**: 2787–2791.
59. Goldberg DE. *Genetic Algorithms in Search, Optimization and Machine Learning*. Addison-Wesley Pub. Co., Boston, 1989.